LEVEL

ADA103475

TECHNICAL REPORT ARLCB-TR-81028

STRUCTURAL ANALYSIS OF A KINETIC
ENERGY PROJECTILE DURING LAUNCH

G. A. Pflegl
J. H. Underwood
G. P. O'Hara

Jul 1981

US ARMY ARMAMENT RESEARCH AND DEVELOPMENT COMMAND
LARGE CALIBER WEAPON SYSTEMS LABORATORY
BENÉT WEAPONS LABORATORY
WATERVLIET, N. Y. 12189

DTIC
SELECTED
AUG 3 1 1981

A

81 8 31 120

DTIC FILE COPY

410224

DISCLAIMER

The findings in this report are not to be construed as an official Department of the Army position unless so designated by other authorized documents.

The use of trade name(s) and/or manufacture(s) does not constitute an official indorsement or approval.

DISPOSITION

Destroy this report when it is no longer needed. Do not return it to the originator.

REPORT DOCUMENTATION PAGE		READ INSTRUCTIONS BEFORE COMPLETING FORM
1. REPORT NUMBER ARLCB-TR-81028	2. GOVT ACCESSION NO. AD-A103 475	3. RECIPIENT'S CATALOG NUMBER
4. TITLE (and Subtitle) STRUCTURAL ANALYSIS OF A KINETIC ENERGY PROJECTILE DURING LAUNCH		5. TYPE OF REPORT & PERIOD COVERED
		6. PERFORMING ORG. REPORT NUMBER
7. AUTHOR(s) G. A. Pflegl, J. H. Underwood, and G. P. O'Hara		8. CONTRACT OR GRANT NUMBER(s)
9. PERFORMING ORGANIZATION NAME AND ADDRESS US Army Armament Research & Development Command Benet Weapons Laboratory, DRDAR-LCB-TL Watervliet, NY 12189		10. PROGRAM ELEMENT, PROJECT, TASK AREA & WORK UNIT NUMBERS AMCMS No. 4111.16.2991.0 PRON No. 1A-9-39362-0
11. CONTROLLING OFFICE NAME AND ADDRESS US Army Armament Research & Development Command Large Caliber Weapon Systems Laboratory Dover, NJ 07801		12. REPORT DATE July 1981
		13. NUMBER OF PAGES 18
14. MONITORING AGENCY NAME & ADDRESS(if different from Controlling Office)		15. SECURITY CLASS. (of this report) UNCLASSIFIED
		15a. DECLASSIFICATION/DOWNGRADING SCHEDULE

16. DISTRIBUTION STATEMENT (of this Report)

Approved for public release; distribution unlimited.

17. DISTRIBUTION STATEMENT (of the abstract entered in Block 20, if different from Report)

18. SUPPLEMENTARY NOTES

19. KEY WORDS (Continue on reverse side if necessary and identify by block number)

Penetrator
Sabot
Stress
Fracture

20. ABSTRACT (Continue on reverse side if necessary and identify by block number)

This paper presents the results of a three phase effort to quantify the
structural integrity of a long rod kinetic energy penetrator projectile during
launch. The first phase used the finite element method to investigate the two
body problem of penetrator and sabot during peak launch loads. This portion
of the analysis considered the effect of pressure loading, body forces, and
different moduli to determine an estimate of the stresses present in the
(CONT'D ON REVERSE)

DD FORM 1473 1 JAN 73   EDITION OF 1 NOV 65 IS OBSOLETE

20. ABSTRACT (CONT'D)

penetrator and sabot - particularly along the intersection between the two.
These stresses were then used to determine the lord transfer between the
penetrator and sabot.

The second phase of the effort applied the load transfer from phase one to a
detailed finite element model of the thread-like lugs of the penetrator in order
to determine the stress concentrations in the notch root area between the lugs.
This portion of the work took into account the geometry, material properties,
and load transfer of the lugs. The resulting stresses due to the shearing and
bending loads and contact friction were analyzed to determine the location and
magnitude of the largest tensile stresses at the surface of the lug root.

The value of maximum tensile stress in the root of the penetrator lugs was then
used in a fracture mechanics analysis to determine a critical flow size which
would cause brittle fracture. Using fracture toughness measurements from
depleted uranium penetrator materials, critical flaw sizes were calculated and
used to determine the likelihood of failure during launch and to formulate NDT
inspection standards.

TABLE OF CONTENTS

TABLES

LIST OF ILLUSTRATIONS

1

INTRODUCTION

This program for the structural analysis of a high density penetrator round during launch was initiated by a breakup of a penetrator during firing at low temperature (-50°F) during prototype development of the XM774 round. Flash x-rays of the XM774 round as it exited the muzzle disclosed that the penetrator had separated into two parts in the region of the rearmost lugs. This failure was unexpected, since the round had performed well in both normal and high temperature firing tests. Summarized here are the results of an investigation to determine the most probable cause of the failure and recommending changes to avoid such a failure in the future.
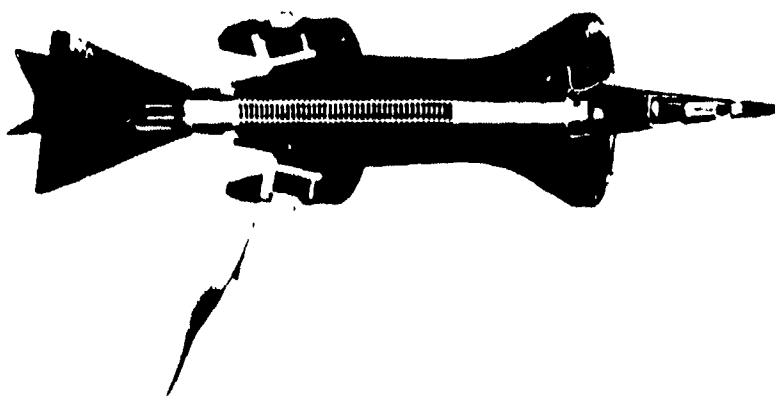

Figure 1. A typical kinetic energy penetrator round (one sabot section removed).

The round involved is used with the 105 mm M68 tank gun. It has a fin stabilized long rod penetrator of depleted uranium -0.75% titanium alloy carried by a 7075-T6 aluminum sabot. Figure 1 is a picture of such a round with one of the three sabot segments removed to show the detail of the lug interconnection.

THE APPROACH

The fact that a penetrator failed during cold temperature testing rather than at normal or high temperature firings is an indication of a brittle failure that can be described by fracture mechanics, providing that stresses are known. A three phase approach was taken towards identifying and quantifying this low temperature, brittle failure. The first phase was a finite element model of the entire penetrator and sabot assembly. This model took into account the geometries of the components, the loading by gas pressure and body force, and the different engineering material properties. The results of this phase were the stress fields due to launch loads for both the penetrator and the sabot, and the load transfer values along the penetrator-sabot interface, which became the input for the second section of the analytical effort.

The second phase of the work concentrated on the lugs machined on the penetrator and their interaction with the similar lugs on the inside of the sabot. Taken into account here were the geometry, engineering material properties, the stresses in the underlying material, and the load transfer applied to the surface of the lugs as normal and friction forces. The results were the determination of the location, orientation and magnitude of the tensile stress concentrations at the root of the lugs at the rear of the

2

penetrator. This portion of the study also provided an assessment of the load transfer capabilities of the lugs and how they can be improved.

The third phase of the analysis used the value of maximum tensile stress in the root of the lugs along with the measured fracture toughness of the penetrator material at low temperature to determine the critical crack size above which brittle failures would be expected during test firings. This final step leads to the requirements for material fracture toughness of the penetrator blanks and for NDT standards of the finish machined product.

The three step plan of analysis provided some understanding of why the penetrator broke during launch and how to prevent such problems from reoccurring. Also, and perhaps just as important, it has provided a comprehensive method for investigating other rounds of this type in such a way that it will identify most problem areas.

PENETRATOR-SABOT ANALYSIS

The analysis of the penetrator and sabot was conducted using the finite element method of the NASTRAN program. It is beyond the scope of this paper to explain either the method or the program. Those readers who wish further information on the subject can consult reference 1 and 2 or other of the many publications on the subject. NASTRAN was chosen not only because of its availability and the familiarity of the investigators with it, but also because it could handle the many facets of this multi-bodied problem.

---

[1]O. C. Zienkiewicz, The Finite Element Method, Third Edition, McGraw-Hill 1977.
[2]R. H. MacNeal, "The NASTRAN Theoretical Manual," NASA SP-221(04), December 1977.

3

The analysis used axisymmetric ring elements to represent the DU material of the penetrator, the aluminum sabot, and the RTV seal at the base of the sabot. Figure 2 is a cross section of the structure which shows the detail and accuracy attainable with the grid generation program. Only the threads for the fin assembly and the lugged connection were not detailed. To do so would have added to the expense with little increase in return because of the three step nature of the analytical procedure. The diameter of the model in these two areas was set at the pitch diameter, which resulted in the weights of the modeled components deviating less than one percent from the average measured values. The weights of the additional components (fins, nose cones, etc.) were represented by lumped masses located at appropriate mesh points.

The loading of the penetrator-sabot model was accomplished by applying a set of forces to the rear surfaces of the penetrator, RTV sealant, and sabot (up to the obturating band) which represented the peak projectile base pressure for $-50°F$ firings; i.e., 32,680 psi. The fact that the pressure effect was applied directly to the rear of the penetrator and not to the fin assembly is of little consequence because the net effect on the projectile ahead of the fins is the same and the stresses in the fin region are too low to warrant concern. The inertial forces due to acceleration were applied to all points of the projectile with a magnitude equivalent to the peak value experienced during launch at low temperature; i.e., 34,360 g's. The force balance of the system was effected by constraining the forward surface of the obturating band groove of the sabot in the axial direction. This is the same surface upon which the net force of the obturating band acts during firing.

4
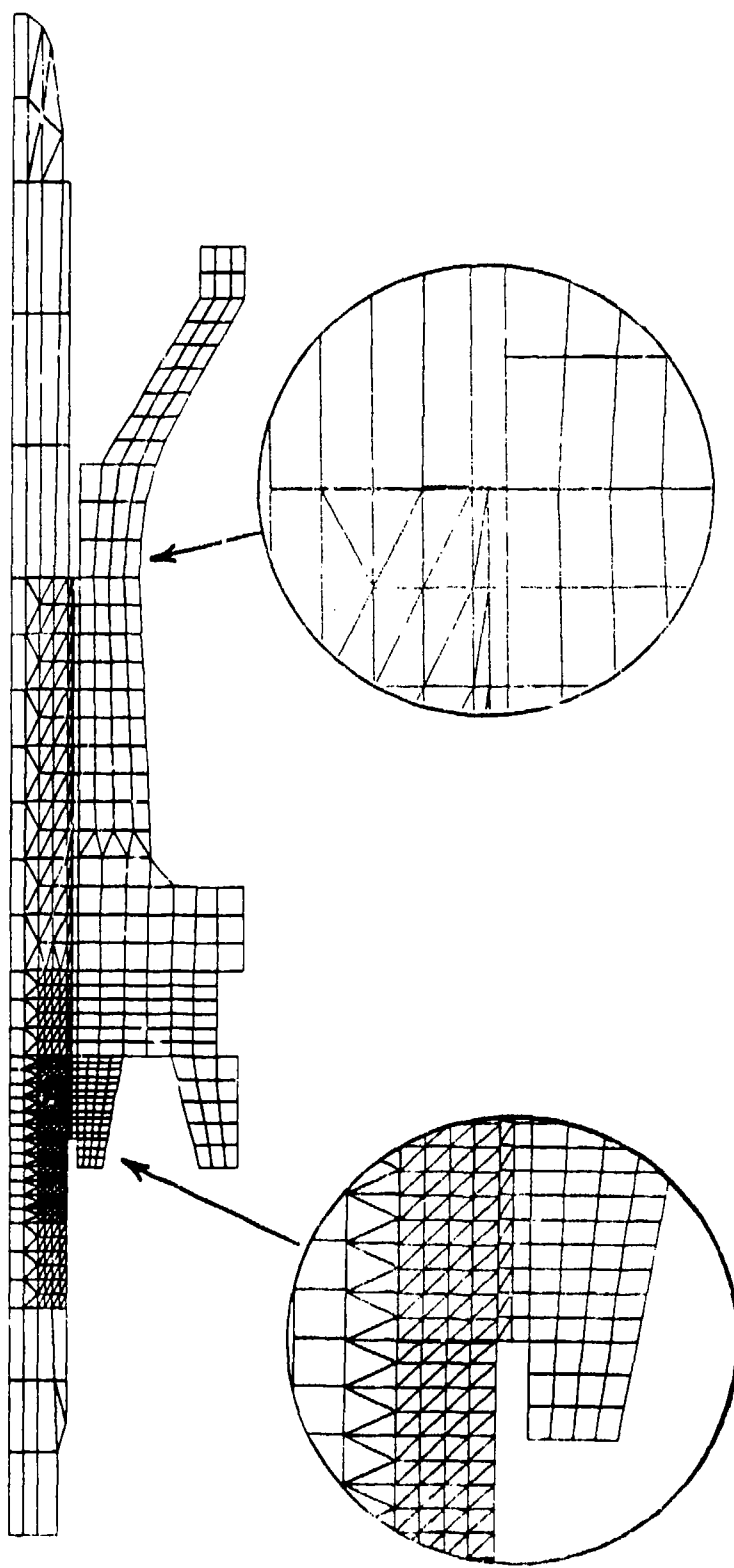
Figure 2. Finite element mesh of penetrator and sabot.

Consideration of the NASTRAN results concentrated on the output related to the penetrator, since this was the item of most immediate concern. Processing of the NASTRAN output showed two areas of elevated octahedral shear stress. These regions are indicated on Figure 2 as areas A and B. Area A is that portion of the penetrator adjacent to the forward end of the sabot. Compressive axial stresses are highest here because the material must support all of the front projectile overhang against the inertial body forces. This could lead to buckling if the penetrator overhang is too great or improperly supported. However, since the stresses are compressive they are of less concern than the tensile stresses toward the rear of the penetrator. Area B has high axial tensile stresses due to the rearward overhang of the penetrator and the discontinuity in surface shear loading at the back of the sabot.

Figures 3 and 4 indicate the sharp gradients in the axial stress as a function of axial and radial position (respectively) within the region. The values of stress used to plot Figure 3 are taken at the centroids of the elements, so that the stresses are somewhat higher on the surface as shown in plot B-B of Figure 4. By extrapolating between the curves of Figure 4, the axial stresses in the penetrator at the roots of the rearmost lugs can be determined. The axial and radial loads on the penetrator lugs can be determined from the values of r-z shear and radial stresses for the lug elements. Table I lists the results of the penetrator-sabot analysis. Note that at fillet A of the rearmost lug, although the axial tensile stress is high, the fillet radius is much larger and there is no load on the lug. So it is expected that fillet B of the rearmost loaded lug will be the critically loaded location of the penetrator.

6
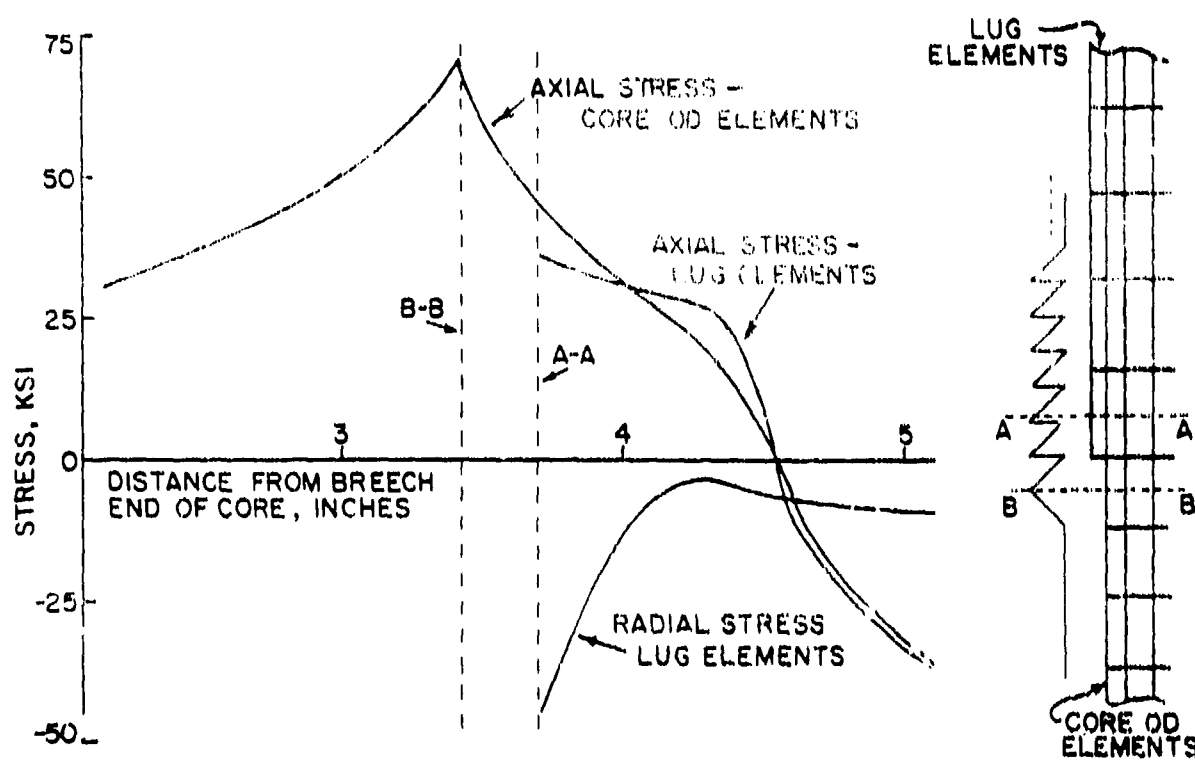
Figure 3. Stress in area B as function of axial position.

7
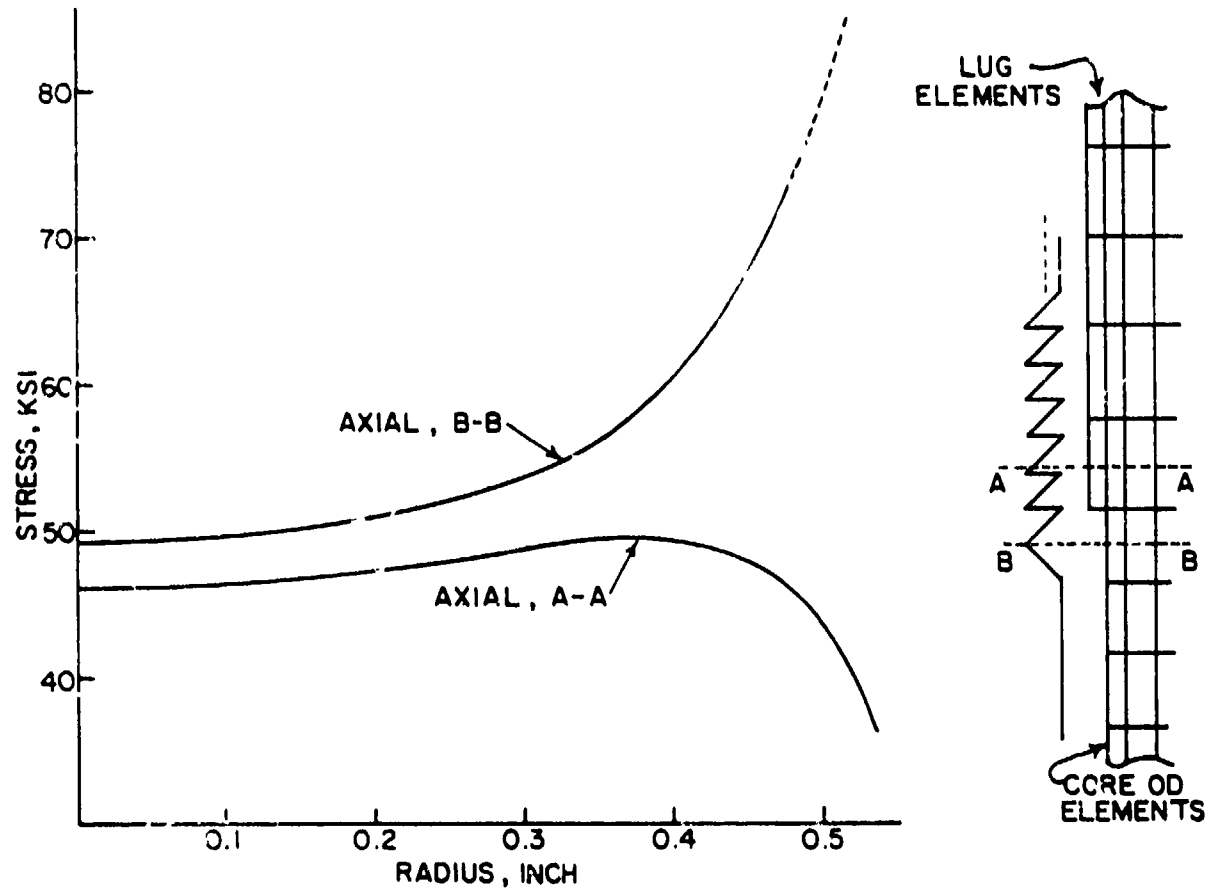
Figure 4. Stress in area B as function of radial position.

8
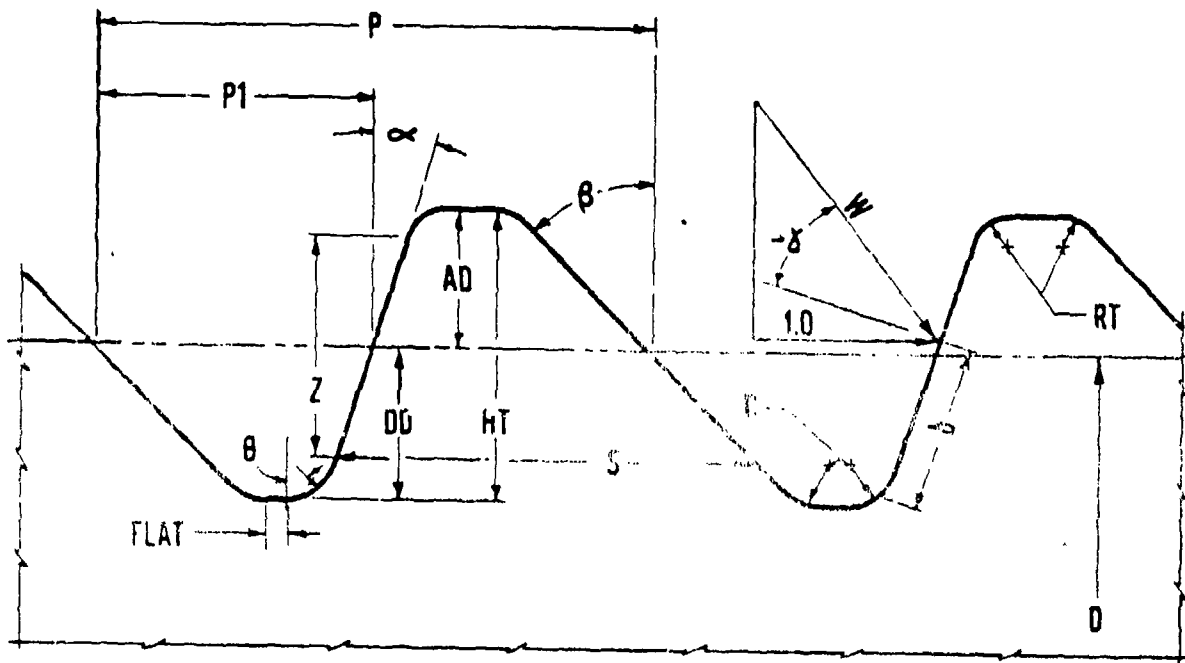
Figure 5. Parameters for lug analysis.

LUG ANALYSIS

The lugs of the penetrator and sabot are like screw threads, having similar cross section and loading but no helix angle. Thus the analysis of the lugs of the penetrator is patterned after nearly identical work done for threads.[3] Threads may fail for several reasons including corrosion, bearing surface failure (wear, galling, push off), shear failure (full or partial engagement) or fillet failure. Some appreciation of the complexity of the

---

[3]C. P. O'Hara, "Finite Element Analysis of Threaded Connections," in Proceedings Army Symposium on Solid Mechanics, Bass River, MA, September 10-12, 1974. (Published by Army Materiel and Mechanics, Watertown, MA.)

thread/lug failure problem can be gained by considering the complex geometry
and dimensions of a typical thread, Figure 5. Since this investigation was
initiated by an apparently brittle failure of the rear of the penetrator, the
analysis was directed toward determining the nature of the fillet stresses in
the rearmost lugs that might lead to failure. Toward this end, it is
necessary to know the effects of loading on the lugs and the associated fillet
stresses. It should be noted again that there are body forces acting on the
projectile along with forces normal and parallel to the lug surfaces.

The material in the fillet (of a notch or step) of a body will be more
highly stressed than the same material would be without the geometric anomaly
whenever there is a stress field induced in the body.[4] The ratio of the
highest stress thus produced to the normally occurring (unnotched) stress is
called the stress concentration factor due to the notch. The magnitude of the
concentration is affected by the radius of the fillet and the depth of the
notch. Figure 6 shows the finite element model of the penetrator lug which
was used to calculate the stresses and stress concentration factor at the lug
fillet. Table I lists the stress concentration factors which were calculated

applied to the axial tensile stresses in the penetrator in the area of the
rearmost lugs.

---

[4]R. E. Peterson, Stress Concentration Factors, John Wiley & Sons, (1974), pp.
26 and 85.
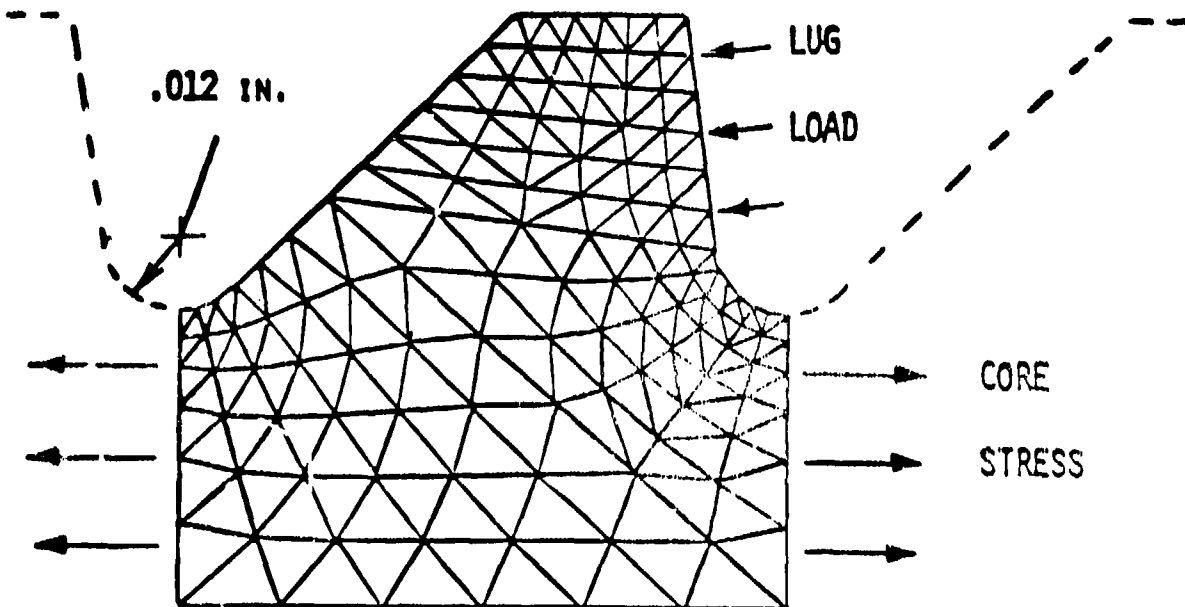
Figure 6. Finite element mesh of lug profile.

The loading on the lug face will also cause a stress rise in the fillet.
The magnitude of the increase will depend upon the geometry of the lug
(height, angles of front and back surfaces, fillet radius, etc.[5]) and upon
the magnitude and ratio of the forces normal and parallel to the lug surfaces.
Load normal to the surface causes bending of the lug which induces tensile
stresses in the fillets. Force parallel to the surface of the lug is
maintained by the friction between the penetrator and the sabot. This force

---

[5]G. P. O'Hara, "Stress Concentrations in Screw Threads," ARRADCOM Technical
Report, ARLCB-TR-80010, Benet Weapons Laboratory, Watervliet, NY (1980).

11

can be negative or positive depending upon whether the radial force is directed inward or outward, respectively. It is also a function of the normal force and the coefficient of friction (about 0.5 for this case). For the penetrator under consideration the force is directed radially inward and as such produces compressive stresses in the fillet which tend to reduce the tensile stress of the bending load. It should be noted that the stress distributions produced by the two methods of lug loading are different and therefore the values of peak stress can not be added directly. Table I summarizes the lug loading factors and the resultant stresses in the fillets.

The results of the lug analysis include the magnitude, location and orientation of the highest tensile stresses on the surfaces of the lug fillets. However, the combined penetrator-sabot and lug analyses provide other information which may be important in considering the integrity of the penetrator. The most important consideration is that there are very high spatial rates of change of the stresses in the fillets, particularly in the radial direction. Therefore, although stresses are high on the surface of the fillets, they drop off rapidly with depth into the material of the penetrator. This means that regions of high stress are "well contained" in the fillet regions and will not lead to gross failure even when indicated values of stress are above the ultimate strength providing there are no cracks present in the region. In fact, of course, the stresses are not expected to exceed the ultimate strength, as has been shown by recent elastic-plastic finite element results.[6]

------

[6]G. P. O'Hara, "Elastic-Plastic Analysis of Screw Threads," ARRADCOM Technical Report, ARLCB-TR-80043, Benet Weapons Laboratory, Watervliet, NY (1980).

FRACTURE ANALYSIS

The fracture mechanics analysis is based on the assumption of a crack being present at the point of highest tensile stress concentration in the fillet of the lugs. The expression for stress intensity factor for a crack in a tensile stress field is of the form

$$K_I = f \sqrt{\pi a} \qquad (1)$$

where a is the crack depth and σ is the tensile stress normal to the crack. The crack geometry factor f for this problem is a function of the crack depth, a, relative to the penetrator radius, r, and the length of the crack along the fillet, 2c. For the relatively small values of a/r expected for this case (up to 0.05) and for a value of a/2c = 0.3 which is typical of many natural flaws, the value of f is 0.83.[7,8]

Using the above value of f and rearranging equation (1), the expression for critical crack size, a_c, at the lug fillet is

$$a_c = 0.462 (\frac{K_{Ic}}{\sigma_f})^2 \qquad (2)$$

where K_{Ic} is the plane strain fracture toughness of the penetrator material and σ_f is the axial tension stress in the lug fillet. Table I shows calculations of a_c using K_{Ic} values of 21.8 Ksi$\sqrt{in}$, the mean of nine K_{Ic} measurements taken at -50°F during the development of the XM774 round and 30 Ksi$\sqrt{in}$, the current specified minimum value of -50° K_{Ic} for the M774

---

[7]H. Tada, P. C. Paris, and G. R. Irwin, The Stress Analysis of Cracks Handbook, Del Research Corporation, Hellerstown, PA (1973).
[8]A. S. Kobayashi, and W. L. Mass, Fracture, P. L. Pratt, Ed., Chapman and Hall, Ltd., London (1969).

13

production material. Note first that the increase in toughness from 21.8 to 30 Ksi$\sqrt{in}$ nearly doubles the critical crack size which can be present before failure is expected. In addition, the a_c value calculated from equation (2) using an elastic plastic calculation of fillet stress[6,9] $\sigma_F \cong 170$, and K_{Ic} = 30 Ksi$\sqrt{in}$, is 0.014 inch. These a_c calculations were used to establish the minimum allowed K_{Ic} value and the maximum allowed NDT defect sizes for the M774 penetrator material.

SUMMARY

The launch failure of a DU alloy penetrator during test firings at -50°F of the XM774 105 mm round started a three phase investigation to determine the most probable cause of the failure and a means of preventing it in the future. The first phase of the investigation was a finite element analysis of the complete round to determine areas of high stress. This analysis identified the area of the penetrator adjacent to the forward end of the sabot as a region of high compressive stress. It also identified the material near the surface of the penetrator and adjacent to the rear of the sabot as having high tensile axial stress. This is the location at which the penetrator failed during launch. These high stresses (see Table I) occur at the base of the rearmost lugs connecting the penetrator to the sabot.

The second phase of the investigation applied this axial stress to a finite element model of a single penetrator lug. The axial and radial

[6]G. P. O'Hara, "Elastic-Plastic Analysis of Screw Threads," ARRADCOM Technical Report, ARLCB-TR-80043, Benet Weapons Laboratory, Watervliet, NY (1980).
[9]"Report of 105 mm, APFDS, XM774 Transition Committee," ARRADCOM Technical Report portions classified (July 1980).

TABLE I. SUMMARY OF STRESS AND FRACTURE ANALYSIS

	Fillet A	Fillet ᵖ	Fillet B
radius:	0.62"	.010"	.005"
Part 1: Penetrator-Sabot Analysis			
Axial Stress	85 Ksi	60 Ksi	60 Ksi
Radial Load	0	31.1 Ksi	31.1 Ksi
Shear Transfer Load	0	31.6 Ksi	31.6 Ksi
Part 2: Lug Analysis			
Stress Concentration Factor	1.2	2.0	2.5
Concentrated Stress	102 Ksi	120 Ksi	150 Ksi
Lug Load Stress	0	98 Ksi	135 Ksi
Highest Total Axial Stress, σ_F	102 Ksi	218 Ksi	285 Ksi
Part 3: Fracture Mechanics Analysis			
Critical Crack Depth			
For $K_{Ic} = 21.8$	.021 in.	.005 in.	-
For $K_{Ic} = 30$	.040 in.	.009 in.	-

Penetrator

A   B

Sabot

interface loads determined from the first phase were applied to the pressure faces of the lugs. These loads were divided into components perpendicular and parallel to the surfaces and represented the normal and friction forces. The stress concentrations in the lug fillet due to the notch and bending effects of the lug greatly increased the tensile stress in the fillet. The stress concentration for the friction loads directed radially inward tended to reduce the stress in the fillet. Table I shows the individual component and total stresses for the two rearmost fillets of the penetrator lugs.

The third phase of the investigation used the calculated values of maximum tensile fillet stress and measured values of the fracture toughness of the alloy to calculate the critical crack size in the fillets of the rearmost lugs. The calculated critical crack sizes were used to establish the minimum allowed K_{Ic} value and the maximum allowed NDT defect sizes for production and inspection of M774 DU alloy penetrators.

REFERENCES

1. O. C. Zienkiewicz, The Finite Element Method, Third Edition, McGraw-Hill (1977).

2. R. H. MacNeal, The NASTRAN Theoretical Manual, NASA SP-221(04), (December 1977).

3. G. P. O'Hara, "Finite Element Analysis of Threaded Connections," in Proceedings Army Symposium on Solid Mechanics, Bass River, MA, September 10-12, 1974. (Published by Army Material and Mechanics, Watertown, MA).

4. R. E. Peterson, Stress Concentration Factors, p. 26 and 85. John Wiley & Sons (1974).

5. G. P. O'Hara, "Stress Concentrations in Screw Threads," ARRADCOM Technical Report, ARLCB-TR-80010, Benet Weapons Laboratory, Watervliet, NY (1980).

6. G. P. O'Hara, "Elastic-Plastic Analysis of Screw Threads," ARRADCOM Technical Report, ARLCB-TR-80043, Benet Weapons Laboratory, Watervliet, NY (1980).

7. H. Tada, P. C. Paris, and G. R. Irwin, The Stress Analysis of Cracks Handbook, Del Research Corporation, Hellerstown, PA (1973).

8. A. S. Kobayashi, and W. L. Mass, Fracture 1969, P. L. Pratt, Ed., Chapman and Hall, Ltd., London (1969).

9. "Report of 105 mm, APFDS, XM774 Transition Committee," ARRADCOM Technical Report, portions classified (July 1980).

TECHNICAL REPORT INTERNAL DISTRIBUTION LIST

	NO. OF COPIES
COMMANDER	1
CHIEF, DEVELOPMENT ENGINEERING BRANCH	1
ATTN: DRDAR-LCB-DA	1
-DM	1
-DP	1
-DR	1
-DS	1
-DC	1
CHIEF, ENGINEERING SUPPORT BRANCH	1
ATTN: DRDAR-LCB-SE	1
-SA	1
CHIEF, RESEARCH BRANCH	2
ATTN: DRDAR-LCB-RA	1
-RC	1
-RM	1
-RP	1
CHIEF, LWC MORTAR SYS. OFC.	1
ATTN: DRDAR-LCB-M	
CHIEF, IMP. 81MM MORTAR OFC.	1
ATTN: DRDAR-LCB-I	
TECHNICAL LIBRARY	5
ATTN: DRDAR-LCB-TL	
TECHNICAL PUBLICATIONS & EDITING UNIT	2
ATTN: DRDAR-LCB-TL	
DIRECTOR, OPERATIONS DIRECTORATE	1
DIRECTOR, PROCUREMENT DIRECTORATE	1
DIRECTOR, PRODUCT ASSURANCE DIRECTORATE	1

NOTE: PLEASE NOTIFY ASSOC. DIRECTOR, BENET WEAPONS LABORATORY, ATTN: DRDAR-LCB-TL, OF ANY REQUIRED CHANGES.

TECHNICAL REPORT EXTERNAL DISTRIBUTION LIST

	NO. OF COPIES		NO. OF COPIES
ASST SEC OF THE ARMY RESEARCH & DEVELOPMENT ATTN: DEP FOR SCI & TECH THE PENTAGON WASHINGTON, D.C. 20315	1	COMMANDER US ARMY TANK-AUTMV R&D COMD ATTN: TECH LIB - DRDTA-UL MAT LAB - DRDTA-RK WARREN MICHIGAN 48090	1 1
COMMANDER US ARMY MAT DEV & READ. COMD ATTN: DRCDE 5001 EISENHOWER AVE ALEXANDRIA, VA 22333	1	COMMANDER US MILITARY ACADEMY ATTN: CHMN, MECH ENGR DEPT WEST POINT, NY 10996	1
COMMANDER US ARMY ARRADCOM ATTN: DRDAR-LC -LCA (PLASTICS TECH EVAL CEN) -LCE -LCM -LCS -LCW -TSS(STINFO) DOVER, NJ 07801	1 1 1 1 1 1 2	COMMANDER REDSTONE ARSENAL ATTN: DRSMI-RB -RRS -RSM ALABAMA 35809	2 1 1
		COMMANDER ROCK ISLAND ARSENAL ATTN: SARRI-ENM (MAT SCI DIV) ROCK ISLAND, IL 61202	1
COMMANDER US ARMY ARRCOM ATTN: DRSAR-LEP-L ROCK ISLAND ARSENAL ROCK ISLAND, IL 61299	1	COMMANDER HQ, US ARMY AVN SCH ATTN: OFC OF THE LIBRARIAN FT RUCKER, ALABAMA 36362	1
DIRECTOR US Army Ballistic Research Laboratory ATTN: DRDAR-TSB-S (STINFO) ABERDEEN PROVING GROUND, MD 21005	1	COMMANDER US ARMY FGN SCIENCE & TECH CEN ATTN: DRXST-SD 220 7TH STREET, N.E. CHARLOTTESVILLE, VA 22901	1
COMMANDER US ARMY ELECTRONICS COMD ATTN: TECH LIB FT MONMOUTH, NJ 07702	1	COMMANDER US ARMY MATERIALS & MECHANICS RESEARCH CENTER ATTN: TECH LIB - DRXMR-PL WATERTOWN. MASS 02172	2
COMMANDER US ARMY MOBILITY EQUIP R&D COMD ATTN: TECH LIB FT BELVOIR, VA 22060			

NOTE: PLEASE NOTIFY COMMANDER. ARRADCOM, ATTN: BENET WEAPONS LABORATORY, DRDAR-LCB-TL, WATERVLIET ARSENAL, WATERVLIET, N.Y. 12189, OF ANY REQUIRED CHANGES.

TECHNICAL REPORT EXTERNAL DISTRIBUTION LIST (CONT)

	NO. OF COPIES		NO. OF COPIES
COMMANDER US ARMY RESEARCH OFFICE P.O. BOX 12211 RESEARCH TRIANGLE PARK, NC 27709	1	COMMANDER DEFENSE TECHNICAL INFO CENTER ATTN: DTIA-TCA CAMERON STATION ALEXANDRIA, VA 22314	12
COMMANDER US ARMY HARRY DIAMOND LAB ATTN: TECH LIB 2800 POWDER MILL ROAD ADELPHIA, MD 20783	1	METALS & CERAMICS INFO CEN BATTELLE COLUMBUS LAB 505 KING AVE COLUMBUS, OHIO 43201	1
DIRECTOR US ARMY INDUSTRIAL BASE ENG ACT ATTN: DRXPE-MT ROCK ISLAND, IL 61201	1	MECHANICAL PROPERTIES DATA CTR BATTELLE COLUMBUS LAB 505 KING AVE COLUMBUS, OHIO 43201	1
CHIEF, MATERIALS BRANCH US ARMY R&S GROUP, EUR BOX 65, FPO N.Y. 09510	1	MATERIEL SYSTEMS ANALYSIS ACTV ATTN: DRXSY-MP ABERDEEN PROVING GROUND MARYLAND 21005	1
COMMANDER NAVAL SURFACE WEAPONS CEN ATTN: CHIEF, MAT SCIENCE DIV DAHLGREN, VA 22448	1		
DIRECTOR US NAVAL RESEARCH LAB ATTN: DIR, MECH DIV CODE 26-27 (DOC LIB) WASHINGTON, D. C. 20375	1 1		
NASA SCIENTIFIC & TECH INFO FAC P. O. BOX 8757, ATTN: ACQ BR BALTIMORE/WASHINGTON INTL AIRPORT MARYLAND 21240	1		

NOTE: PLEASE NOTIFY COMMANDER, ARRADCOM, ATTN: BENET WEAPONS LABORATORY,
DRDAR-LCB-TL, WATERVLIET ARSENAL, WATERVLIET, N.Y. 12189, OF ANY
REQUIRED CHANGES.